[Article] www.whxb.pku.edu.cn

射频等离子体技术制备合成低碳醇用新型 Cu-Co/SiO_2 催化剂

徐慧远 储 伟* 邓思玉
(四川大学化工学院, 成都 610065)

摘要: 采用射频等离子体技术制备新型 Cu-Co/SiO_2 催化剂. 与直接焙烧制备的样品相比, 射频等离子体处理提高了催化剂的比表面积, 显著增大了活性物种 Co 的表面含量, 有效改进了催化剂的还原性能. 以 CO 加氢合成低碳混合醇为模型反应, 在 563 K, 5.0 MPa, 6000 h^{-1}, $V(H_2)$:$V(CO)$=1.6 的条件下, 等离子体处理和等离子体处理后再焙烧样品比 673 K 焙烧样品的催化活性提高 30.46%和 65.30%, 低碳醇的时空收率分别提高 58.22%和 76.11%.

关键词: 射频等离子体; 一氧化碳加氢; 铜钴基催化剂; 低碳醇
中图分类号: O643

Preparation of Copper-Cobalt-Silicon Catalysts for Higher Alcohol Synthesis by Glow Discharge Plasma

XU Hui-Yuan CHU Wei* DENG Si-Yu
(*College of Chemical Engineering, Sichuan University, Chengdu 610065, P. R. China*)

Abstract: Novel Cu-Co/SiO_2 catalysts were prepared by conventional impregnation methods with the assistance of glow discharge plasma technology. Compared with a conventional calcined sample, the plasma remarkably improved the specific surface area of the catalyst and increased the concentration of active cobalt species on the catalyst's surface. The reducibility of the cobalt was effectively improved as well. Catalytic test results showed that comparison to the conventional 673 K calcined sample, the CO hydrogenation activity of the two plasma enhanced samples (one treated only by plasma and the other assisted by plasma followed by calcination) increased by 30.46% and 65.30%, respectively. Their time space yields of higher alcohols also increased by 58.22% and 76.11%, respectively, under 5.0 MPa, 6000 h^{-1}, 563 K and a H_2/CO volume ratio of 1.6.

Key Words: Glow discharge plasma; CO hydrogenation; Copper-cobalt based catalyst; Higher alcohol

Cu-Co based catalysts are considered as one of the most promising catalyst systems for the synthesis of higher alcohols[1–10]. The application of this technology is mainly determined by the development of catalyst with excellent performance[1,7,9–10]. In plasma field, there are full of energetic species, such as ions, electrons, and free radicals. The thermal effects and chemical effects of these species could modify the interaction between supports and active components. They were widely used for the activation of reactant molecules, and the modification and strengthening preparation of the catalysts[11–20]. The glow discharge plasma assisted Co/Al_2O_3 catalyst showed much higher catalytic performance in Fischer-Tropsch synthesis, the cobalt dispersion was significantly enhanced, and the number of active cobalt sites were increased[11–12]. Liu *et al*.[13–14] focused on the effects of pretreatment with glow discharge plasma on Pd/HZSM-5 catalyst. They found that both the dispersion and acidity of the catalyst were enhanced, the reaction temperature for methane catalytic combustion was evidently decreased, and the stability of the catalyst was improved. The plasma assisted Ni-based catalyst and Ni-Fe based catalyst were prepared by the same methods mentioned in references[15–17], the low-temperature reaction activity and stability were improved. These results suggested that the

Received: September 29, 2009; Revised: December 8, 2009; Published on Web: December 31, 2009.
*Corresponding author. Email: chuwei65@yahoo.com.cn; Tel: +86-28-85403836.
The project was supported by the National Natural Science Foundation of China (20590363).
国家自然科学基金(20590363)资助项目

plasma treatment could effectively improve the activity of supported metal catalysts. Therefore, glow discharge plasma had a wide promising application in catalyst preparation.

Since glow discharge plasma belongs to a kind of non-thermal plasma, it owns high electron temperature (10000–100000 K) and relatively low gas temperature. In this special condition, the catalyst crystal structure can be avoided to damage at high temperature, meanwhile, the integrate force between the active component and support can be changed. Therefore, the catalytic performance can be effectively improved.

In our previous work, Cu-Zn-Al based catalysts for the methanol synthesis[18] and Cu-Co-Zr based catalysts for the synthesis of higher alcohols[19] were prepared and modified with glow-discharge plasma. In this article, we mainly focused on the effects of catalyst pretreated with glow discharge plasma. The catalytic performmance, catalyst crystal structures, surface elements as well as reducibility of the Cu-Co/SiO_2 catalysts were investigated. The catalysts were characterized by N_2 adsorption/desorption, X-ray diffraction (XRD), H_2-temperature programmed reduction (TPR), Fourier transform infrared (FT-IR) spectrometry, and X-ray photoelectron spectroscopy (XPS).

1 Experimental

1.1 Catalyst preparation

The traditional impregnated method and glow discharge plasma treatment method were adopted to prepare the catalysts. Silica was used as the carrier (Qingdao Haiyang Chemical Co., Ltd.). The mixed solution of $Cu(NO_3)_2\cdot 3H_2O$ (AR, Tianjin Bodi Chemical Co., Ltd.) and $Co(NO_3)_2\cdot 6H_2O$ (AR, Fine Chemical factory, Shandong Yutai sino) was prepared according to a certain percentage. The isometric impregnation method was used to prepare the Cu-Co/SiO_2 catalyst precursor. Parts of the precursor were calcined at 573 K for 4 h in air and obtained the CuCoS-C573 sample; parts of the precursor were calcined at 673 K for 4 h in air and obtained the CuCoS-C673 sample; rests of the precursor were treated by the plasma. The treatment progress was carried in the GP062 DL3 capacitive coupling high frequency plasma generator using the following processing parameters: 60 Pa pressure, 13.56 MHz radio frequency, 100 mA anode current, and 50 mA gate flow. After treating in the atmosphere of nitrogen and hydrogen for 45 min separately, the sample was calcined in air at 573 K for 4 h, and the sample marked as CuCoS-PC. The sample which was treated with plasma but without calcination was recorded as CuCoS-P. The mass percentages of copper and cobalt in these catalysts were 20% and 8%, respectively.

1.2 Characterization methods

The specific surface area of catalysts was determined by nitrogen adsorption isotherms at 77 K, using an automated gas sorption system (Quantachrome NOVA 1000e apparatus). Before the measurement, the samples were degassed in vacuum at 573 K for 3 h in order to remove the humidity. The XRD patterns were recorded on a DX-1000 diffractometer using Cu K_α radiation between 20° and 80° with a continuous mode. The voltage and anode current were 40 kV and 25 mA, respectively, and the scanning rate was 0.06 (°)·s^{-1}. XPS were recorded on a XSAM 800 spectrometer with an Al K_α ($h\nu$=1486.6 eV) X-ray source. Charging effects were corrected by adjusting the binding energy of C 1*s* peak from carbon contamination to 284.6 eV. TPR experiments were carried out in a fixed-bed reactor at atmospheric pressure. Typically, 50 mg sample was loaded, and a mixture of H_2/N_2 ($\phi(H_2)$=5%) with a flow rate of 30 mL·min^{-1} passed through. The temperature of the reactor was increased linearly from 400 to 800 K with a ramping rate of 5 K·min^{-1}. The hydrogen consumption was determined by a thermal conductivity detector (TCD). Infrared tested sample firstly mixed with KBr and fully pressed, then tested in the Bruker Tensor 27 infrared spectrometer.

1.3 Catalytic test

The CO selective hydrogenation to higher alcohol was conducted in a continuous fixed-bed reactor. A stainless steel reactor with 300 mm length and internal diameter of 4 mm was used. 500 mg catalyst was loaded and reduced *in situ* at 593 K for 4 h under a flow of H_2 (30 mL·min^{-1}) prior to each reaction test. After the reactor cooling down to 473 K, the reaction pressure was increased to 5.0 MPa by feeding the syngas ($V(H_2)/V(CO)$=1.6). The weight hourly space velocity (WHSV) was set at 6000 h^{-1}. Then the reaction temperature was increased from 473 to 563 K at a rate of 1 K·min^{-1}. The continuous reaction was performed at 563 K. The outlet gases (H_2, CO, N_2, CO_2, and CH_4) were analyzed on-line by a SC-200 model gas chromatograph with thermal conductivity detector (TCD) equipped with a 601 column. The hydrocarbons were analyzed by flame ionization detector (FID) with a GDX103 column. The liquid products were analyzed by a GC112A gas chromatography with FID and SE-30 capillary column (0.33 mm×30 m). Using methane associated with the products, the conversion rate of CO as well as the selectivity of the products was obtained by the carbon balance calculation.

2 Results and discussion

2.1 Texture of catalysts

Properties of pore structure of different catalysts were listed in Table 1. Specific surface area of the catalysts were calculated by BET method, and pore volume and average pore size were obtained by the BJH method. It can be seen from the Table 1 that with the increase of the calcination temperature, the catalyst surface area and pore volume decreased, and the average pore size increased. This was because the high-temperature heat treatment of the sample leads to the collapsing of parts of the small pore in

Table 1 Texture of various copper-cobalt-silicon catalysts

Catalyst	S_{BET}/($m^2\cdot g^{-1}$)	V_{pore}/($cm^3\cdot g^{-1}$)	d_{pore}/nm
CuCoS-C573	198.4	0.0776	1.37
CuCoS-C673	189.7	0.0672	1.41
CuCoS-P	228.7	0.0940	1.35
CuCoS-PC	231.0	0.0886	1.37

the samples. The plasma treatment could enhance the specific surface area of the catalyst and form micropores. The specific surface areas of the CuCoS-P and CuCoS-PC samples were 20.6% and 21.8% higher than that of the CuCoS-C673 sample, respectively. Larger surface area could bring a higher dispersion of active phase, and result in an enhanced activity of catalyst[13,19]. The pore volume of the plasma treatment samples was augmented, while the pore diameter was minished. This might be due to the migration of metal particles from support vector channel to outer surface by the electrostatic effect of plasma. That means parts of the metal particles attached on the pore wall, which induced the decrease of pore diameter; meanwhile the metal particles were enriched on surface of the support, leading to an increase of pore volume[17]. CuCoS-PC, which was combined with the effects of plasma pretreatment and calcination, exhibited a medium pore volume and pore size distribution.

2.2 Crystal phase analysis of catalysts

XRD patterns of the oxidized samples were presented in Fig.1. Crystal phases of CuO (JCPDS card No.48-1548) and $CuCO_2O_4$ (JCPDS card No.01-1155) were coexisted in all the three catalysts. The diffraction peaks at 2θ of 43.46° and 50.36° attributed to metallic Cu phase (JCPDS card No.65-5840) were detected in CuCoS-P catalyst, since the plasma treatment had some reductive effect. The CuO crystallite sizes were calculated from the width at half maximum of CuO(111) phase (2θ=38.69°) using the Scherrer equation. The plasma treatment showed significant effects on the crystallite size of CuO crystallites. The crystallite size of CuO in CuCoS-C573, CuCoS-C673, CuCoS-P, and CuCoS-PC samples was 15.7, 18.9, 4.7, and 8.6 nm, respectively. The remarkable decrease of CuO crystallite size after plasma treatment was due to the effect of a large number of high-energetic species in the plasma field bombarded on the catalyst surface. It made the catalyst precursor decompose under mild conditions, avoided the destruction of catalyst structure and sintering of crystallite during high temperature calcination[18–20], and thus resulted in an improvement of the dispersion of active components.

2.3 XPS characterization

Table 2 Element analysis of various copper-cobalt-silicon catalysts by XPS

Catalyst	x (%)				x_{Co}/x_{Si}
	Cu	Co	Si	O	
CuCoS-C573	14.95	2.84	21.98	60.24	0.129
CuCoS-P	14.24	5.51	24.12	56.14	0.228
CuCoS-PC	14.91	4.57	19.65	60.87	0.233

To study the effect of plasma treatment on the surface distribution of active components, the samples were first reduced in hydrogen and then transferred into the XPS spectrometer for analysis under the protection of high-purity nitrogen. Surface composition of the samples was summarized in Table 2. The surface Co contents of CuCoS-PC and CuCoS-P increased by 94.01% and 60.92%, respectively, and the surface atomic ratio of cobalt-silicon increased by 76.92%, compared with that of the CuCoS-C573 catalyst. This suggested that plasma treatment led to the enrichment of active Co species and enhancement of the dispersion on the catalyst surface. However, the surface Cu content of CuCoS-PC and CuCoS-P samples did not change significantly.

2.4 H_2-TPR measurement

The influence of plasma treatment on the reducibility of the various catalysts was studied by temperature programmed reduction. The H_2-TPR profiles of conventional calcined and plasma assisted samples were shown in Fig.2. Two reduction peaks were exhibited at 400–800 K. The reduction peak at lower temperature could be attributed to the reduction of small CuO cluster or high dispersed surface CuO particles to metallic Cu. CuO "floated" to the surface was especially prone to the Jahn-Teller effect[21]. During heating process, Cu^{2+} preferential entered into the gap of the octahedral spinel. The electron configuration of Cu^{2+} outer layer was $3d^9$ arrangement. The octahedral sub-lattice was twisted and elongated along the d_2^δ as a result of the Jahn-Teller effect. The rejected lattice oxygen ions moved toward to the Co ions, leading to the redistribution of the charge, and meanwhile the system energy was increased, finally induced CuO "floated" to the surface. The reduction peak at higher temperature was attributed to the reduction of highly-interacted Cu-Co species. The

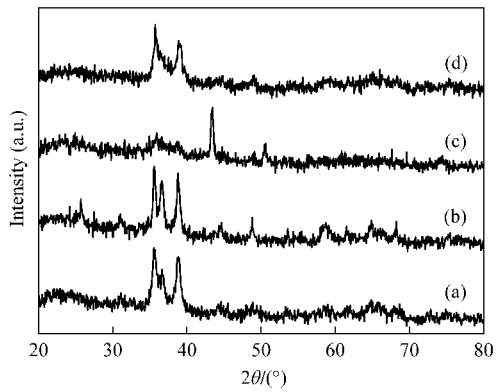

Fig.1 XRD profiles of various copper-cobalt-silicon catalysts

(a) CuCoS-C573, (b) CuCoS-C673, (c) CuCoS-P, (d) CuCoS-PC

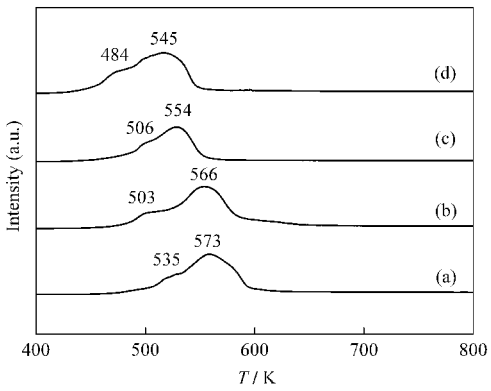

Fig.2 H_2-TPR profiles of various copper-cobalt-silicon catalysts

(a) CuCoS-C573, (b) CuCoS-C673, (c) CuCoS-P, (d) CuCoS-PC

Table 3 Catalytic activity of the catalysts for higher alcohols synthesis from CO+H_2

Catalyst	X_{CO} (%)	S_{ROH} (%)	Y_{ROH}/(g·kg^{-1}·h^{-1})	Product distribution (x, %)				
				MeOH	EtOH	PrOH	BuOH	C_5^+OH
CuCoS-C573	12.82	33.64	75.1	52.59	25.68	11.25	8.97	1.52
CuCoS-C673	14.61	32.90	96.7	46.28	29.62	14.53	7.16	2.41
CuCoS-P	19.06	35.41	153.0	37.41	37.24	14.89	7.71	2.76
CuCoS-PC	24.15	34.54	170.3	36.55	35.38	14.91	10.22	2.94

X: conversion, S: selectivity, Y: space time yield; conditions: 563 K, 5.0 MPa, 6000 h^{-1}, $V(H_2):V(CO)=1.6$

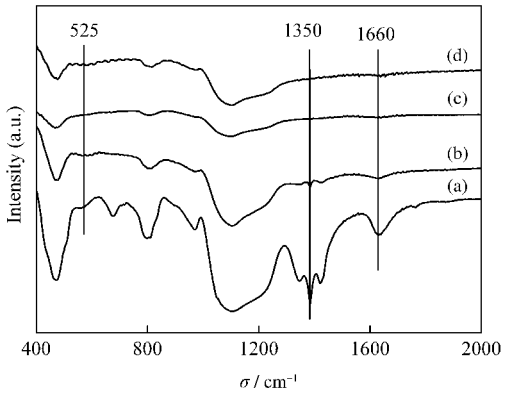

Fig.3 FT-IR spectra of various copper-cobalt-silicon catalysts

(a) CuCoS-C573, (b) CuCoS-C673, (c) CuCoS-P, (d) CuCoS-PC

plasma treatment promoted the reducibility of catalysts evidently. For the CuCoS-C573 sample, the temperature of two reduction peaks were 535 and 573 K. And for the CuCoS-C673 sample, the temperature of two reduction peaks were 503 and 566 K, while in CuCoS-P sample, they were 506 and 554 K, respectively. For CuCoS-PC sample, the temperature of the reduction peaks was the lowest among these three samples, only 484 and 545 K. This may be due to the combined effects of calcination and plasma treatment greatly improving the dispersion of the catalyst. This phenomenon was consistent with the results of catalytic combustion of methane over Pd-based catalysts reported by Liu *et al*.[13].

2.5 FT-IR analysis

FT-IR spectra of these catalysts were shown in Fig.3, the absorption band at around 460 cm^{-1} was assigned to O—Si—O bending vibrations, and the absorption band at around 800 cm^{-1} was attributed to Si—O—Si bending vibrations. The broad band between 1100 and 1200 cm^{-1} corresponded to Si—O—Si stretching vibrations, while the absorption band at 946 cm^{-1} corresponded to stretching vibrations of isolated oxygen groups in Si—O$^-$ [22]. The bands at around 525 and 663 cm^{-1} corresponded to stretching vibrations of Cu—O[23] and Co—O in Co_3O_4[24], respectively. Since the calcination temperature of the CuCoS-C573 sample was lower, the absorption band between 1300 and 1400 cm^{-1} might be attributed to stretching vibrations of N═O, for the incomplete decomposition of nitrate species. The band at 1660 cm^{-1} was assigned to stretching vibrations of adsorbed H_2O[25]. The traditional calcinatied CuCoS-C573 sample and CuCoS-C673 sample showed the characteristic absorption peak of Cu—O at 525 cm^{-1}, which was disappeared in the plasma treatment samples (CuCoS-P, CuCoS-PC), dictated that the crystallite size of the active component was decreased and the dispersion was improved. With the decrease of the crystallite size and the enhancement of the surface area, the cell structure of crystal phase was contracted, and the surface atoms and bulk atoms were in different chemical environment, which resulted in the widening or even disappearance of infrared absorption frequency. The disappearance of bands at around 1300–1400 and 1660 cm^{-1} on the plasma assisted samples showed that the catalyst precursor were completely decomposed by plasma treatment and water was difficult to adsorbed on the plasma assisted samples. The FT-IR results were consistent with the results of XRD and N_2 adsorption desorption, in which the crystallite size of the active component was minished and the surface area was improved by plasma treatment.

2.6 Catalytic performance

The catalytic performance of CO hydrogenation to higher alcohols over the Cu-Co/SiO_2 catalysts was listed in Table 3. As expected, plasma treatment remarkably enhanced the catalytic activity and the space time yield of alcohols. The activity of the plasma treated catalyst (CuCoS-P, CuCoS-PC) was 30.46% and 65.30% higher than that of the conventional calcined CuCoS-C673 sample, and the space time yields of alcohols enhanced by 58.22% and 76.11%, respectively. Combined with the characterizations, it could be conclude that the plasma treatment could decrease the grain size of the active components, enhance the dispersion and increase the number of active sites in the surface of the catalysts. After the introduction of plasma technology, the methanol content in product was decreased, while the content of C_2^+ content in higher alcohols increased significantly. This was due to the enrichment of surface active Co species, which accelerated the formation of CH_x species, and was beneficial to the carbon chain growth, which could be confirmed from the XPS characterization.

3 Conclusions

The thermal effect and chemical effect of glow discharge plasma could effectively promote the interaction between active component and support, and improve the dispersion, the surface concentration as well as the reducibility of the active component. Compared with the traditional calcined catalyst, the activity of CO hydrogenation and the space time yields of alcohols were obviously increased in the plasma treated catalyst.

References

1 Li, D. B.; Ma, Y. G.; Qi, H. J.; Li, W. H.; Sun, Y. H.; Zhong, B. *Prog. Chem*., **2004, 16**: 584 [李德宝, 马玉刚, 齐会杰, 李文怀, 孙玉罕, 钟 炳. 化学进展, **2004, 16**: 584]

2 Sun, X. L.; Roberts, G. W. *Appl. Catal. A*, **2003, 247**: 133

3 Vahid, M.; Mohammad, H. P. *Catal. Commun*., **2006, 7**: 542

4 Vahid, M.; Mohammad, H. P.; Islami, M.; Mehr, J. Y. *Appl. Catal. A*, **2005, 181**: 259

5 Xu, R.; Wei, W.; Li, W. H.; Hu, T. D.; Sun, Y. H. *J. Mol. Catal. A*, **2005, 234**: 75

6 Xu, R.; Ma, Z. Y.; Yang, C.; Wei, W.; Sun, Y. H. *Acta Phys. -Chim. Sin*., **2003, 19**: 423 [徐 润, 马中义, 杨 成, 魏 伟, 孙予罕. 物理化学学报, **2003, 19**: 423]

7 Xu, H. Y.; Chu, W.; Zhou, J. *Industrial Catal*., **2008, 16**: 106 [徐慧远, 储 伟, 周 俊. 工业催化, **2008, 16**: 106]

8 Tien-Thao, N.; Zahedi-Niaki, M. H.; Alamdari, H.; Kaliaguine, S. *J. Catal*., **2007, 245**: 348

9 Xu, X. D.; Doesburg, E. B. M.; Scholten, J. J. F. *Catal. Today*, **1987, 2**: 125

10 Deng, S. Y.; Chu, W.; Xu, H. Y.; Shi, L. M. *J. Natur. Gas Chem*., **2008, 17**: 369

11 Khodakov, A. Y.; Chu, W.; Fongarland, P. *Chem. Rev*., **2007, 107**: 1692

12 Chu, W.; Wang, L. N.; Chernavskii, P. A.; Khodakov, A. Y. *Angew. Chem. Int. Edit.*, **2008, 47**: 5052

13 Liu, C. J.; Yu, K. L.; Zhang, Y. P.; Zhu, X. L.; He, F.; Eliasson, B. *Appl. Catal. B*, **2004, 47**: 95

14 Liu, C. J.; Vissokov, G. P.; Jang, B. W. L. *Catal. Today*, **2002, 72**: 173

15 Liu, G. H.; Li, Y. L.; Chu, W.; Shi, X. Y.; Dai, X. Y.; Yin, Y. X. *Catal. Commun*., **2008, 9**: 1087

16 Zhang, Y.; Chu, W.; Cao, W. M.; Luo, C. R.; Wen, X. G.; Zhou, K. L. *Plasma Chem. Plasma Process.*, **2000, 20**: 137

17 Wang, J. G.; Liu, C. J.; Zhang, Y. P.; Yu, K. L.; Zhu, X. L.; He, F. *Catal. Today*, **2004, 89**: 183

18 Xu, H. Y.; Chu, W.; Ci, Z. M. *Acta Phys. -Chim. Sin*., **2007, 23**: 1042 [徐慧远, 储 伟, 慈志敏. 物理化学学报, **2007, 23**: 1042]

19 Xu, H. Y.; Chu, W.; Shi, L. M.; Zhang, H.; Zhou, J. *Acta Phys. -Chim. Sin*., **2008, 24**: 1085 [徐慧远, 储 伟, 士丽敏, 张 辉, 周 俊. 物理化学学报, **2008, 24**: 1085]

20 Xu, H. Y.; Chu, W.; Shi, L. M.; Zhang, H.; Deng, S. Y. *J. Fuel Chem. Technol.*, **2009, 37**: 212 [徐慧远, 储 伟, 士丽敏, 张 辉, 邓思玉. 燃料化学学报, **2009, 37**: 212]

21 Cai, Q. R.; Peng, S. Y. Catalysis of C1 chemistry. Beijing: Chemical Industry Press, 1995: 520–525 [蔡启瑞, 彭少逸. 碳一化学中的催化作用. 北京: 化学工业出版社, 1995: 520–525]

22 Innocenzi, P. *J. Non-Crystalline Solids*, **2003, 316**: 309

23 Wang, D. J.; Guo, L.; Li, D. S.; Fu, F.; Wang, W. L.; Yan, H. T. *Spectroscopy and Spectral Analysis*, **2008, 28**: 788 [王丹军, 郭 莉, 李东生, 付 峰, 王文亮, 闫洪涛. 光谱学与光谱分析, **2008, 28**: 788]

24 Jiu, J. T.; Ge, Y.; Li, X. N.; Nie, L. *Mater. Lett*., **2002, 54**: 260

25 Zou, G. F.; Li, H.; Zhang, D. W. *J. Phys. Chem. B*, **2006, 110**: 1632